Supporting Information

Inhibition mechanism of melanin formation based on antioxidant scavenging reactive oxygen species

Wencai Fu[a], Zhifang Wu[a], Rui Zheng[a], Na Yin[a], Fangjie Han[a], Zhengzheng Zhao[a], Mengjiao Dai[b], Dongxue Han[a]*, Wei Wang [a]*, Li Niu[a]

[a] Center for Advanced Analytical Science, School of Chemistry and Chemical Engineering c/o School of Civil Engineering, Guangzhou University, Guangzhou 510006, P. R. China;

[b] Guangdong Provincial Key Laboratory of Psychoactive Substances Monitoring and Safety，Anti-Drug Tethnology Center of Guangdong Province, Guangzhou 510230, PR China.

[c] State Key Laboratory of Electroanalytical Chemistry, Changchun Institute of Applied Chemistry, Chinese Academy of Sciences, Changchun 130022, China.

*Address correspondence to: dxhan@gzhu.edu.cn (DX. Han), wangw@gzhu.edu.cn (W. Wang)

Experimental section	Reagents and Materials; Apparatus;
Fig. S1	Adsorption of L-DOPA by TiO_2
Fig. S2	Survival, hatching and malformation rate.
Fig. S3	Quantitative analysis of inhibition of melanin formation by GSH and PG in zebrafish
Fig. S4	Zebrafish melanin repair by itself at day-night.
Table S1	Reagent list of standard Curve
Table S2	L-DOPA in actual samples
Table S3	Effects of antioxidants GSH and PG on acute toxicity, developmental toxicity and teratogenicity of zebrafish embryos
Fig. S5.	Schematic representation of the melanogenesis pathway for eumelanin and pheomelanin.
Fig.S6	HPLC of standard curve of L-DOPA
Fig.S7	In vitro simulation of melanin production
Fig.S8	Effects of different wavelength light sources on melanin formation rate under air saturation, oxygen saturation and nitrogen saturation conditions
Fig.S9	Schematic diagram showing different valence and conduction band for Metal, Semiconductor, and insulating materials.
Fig.S10	General mechanism of TiO_2 in solar photocatalysis process

This material includes:

EXPERIMENTAL SECTION

Reagents and Materials

L-Tyrosine (L-Tyr, 99%), L-DOPA (98%), 9, 10-Diphenyl-anthracene (DPA, 98%), Coumarin (98%) were obtained from Beijing InnoChem (Beijing, China). 1-Phenylthiourea (PTU) was purchased from Bide Pharmatech (Shanghai, China). Titanium dioxide, ascorbic acid (AA, 99%), gallic acid (GA, 99%), L-Glutathione (GSH, 99%), propyl gallate (PG), tyrosinase from mushroom, butylated hydroxyanisole (BHA), 2, 6-Di-tert-butyl-4-methylphenol (BHT) were obtained from Aladdin (Shanghai, China). Wild-type AB zebrafish used were from Institute of Hydrobiology, Chinese Academy of Sciences. The PBS buffer was made from sodium phosphate (NaH_2PO_4/Na_2HPO_4, 81:19 (molar ratio)) and sodium chloride, which were dissolved in deionized water at final concentration of 10 mM (pH 7.4).

Instruments and characterization

UV-1780 (Shimadzu, Japan), HPLC-L600 (Beijing Persee, China), F-4600 (Hitachi, Japan).

Table S1. Reagent list of standard Curve

Volume \ Number	0	1	2	3	4	5	6
NO_2^- standard solution	0	0.2	0.4	0.8	1.2	1.6	2.0
H_2O	2.0	1.8	1.6	1.2	0.8	0.4	0
p-amino-benzenesulfonic acid	2.0	2.0	2.0	2.0	2.0	2.0	2.0
α-naphthylamine	2.0	2.0	2.0	2.0	2.0	2.0	2.0

Table S2. HPLC investigations of standard L-DOPA and L-tyrosine catalysis system

C (μg/mL)	Retention Time	Peak area
0.006	9.067	18503.8
0.008	9.000	24305.6
0.01	7.567	110175.3
0.05	7.367	155774
0.1	7.350	310305
0.2	7.350	484700.5
0.4	7.350	1128449.3
0.6	7.367	1780525.6
0.8	7.383	2361687.00
1.0	7.400	2909640.3
Sample	8.517	19399.9

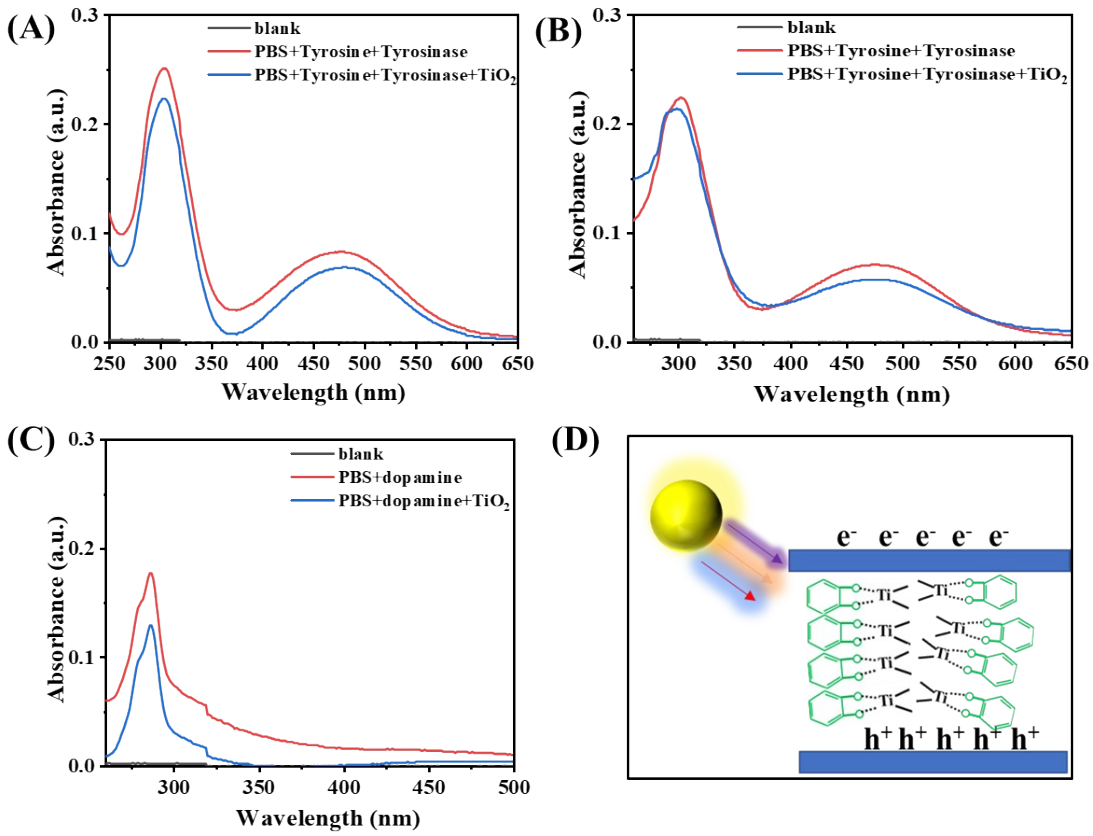

Fig. S1. Adsorption of L-DOPA by TiO_2. (A) The adsorption by TiO_2 of the product in reaction system on the dark condition. (B) The adsorption by TiO_2 of the product in reaction system on the light condition. (C) The adsorption by TiO_2 of L-DOPA standard on the dark condition. (D) Mechanism diagram of dopa adsorption by TiO_2.

Table. S3. Effects of antioxidants GSH and PG on acute toxicity, developmental toxicity and teratogenicity of zebrafish embryos (Compared with the BC：*p＜0.05；**p＜0.01；***p＜0.001)

GSH	BC	2.5 mM	5 mM	10 mM	20 mM	40 mM
Survival rate	100.0±0.0	100.0±0.0	83.3±5.5 ***	0.0±0.0 ***	0.0±0.0 ***	0.0±0.0 ***
	100.0±0.0	100.0±0.0	83.3±5.5 ***	0.0±0.0 ***	0.0±0.0 ***	0.0±0.0 ***
	100.0±0.0	100.0±0.0	83.3±5.5 ***	0.0±0.0 ***	0.0±0.0 ***	0.0±0.0 ***
Hatching rate	0.0±0.0	0.0±0.0	0.0±0.0	0.0±0.0	0.0±0.0	0.0±0.0
	0.0±0.0	2.1±2.1	0.0±0.0	0.0±0.0	4.2±2.1	6.3±3.6

					*	*
	95.8±4.2	100.0±0.0 *	0.0±0.0 ***	0.0±0.0 ***	0.0±0.0 ***	0.0±0.0 ***
	0.0±0.0	0.0±0.0	33.3±5.5 ***	100.0±0.0 ***	100.0±0.0 ***	100.0±0.0 ***
Malformation rate	0.0±0.0	2.1±2.1	16.7±5.5 ***	100.0±0.0 ***	100.0±0.0 ***	100.0±0.0 ***
	0.0±0.0	4.2±2.1	16.7±5.5 ***	100.0±0.0 ***	100.0±0.0 ***	100.0±0.0 ***
PG	BC	0.0625 mM	0.125 mM	0.25 mM	0.5 mM	1.0 mM
Survial rate	100.0±0.0	100.0±0.0	100.0±0.0	97.9±2.1	100.0±0.0	95.8±4.2
	100.0±0.0	100.0±0.0	100.0±0.0	97.9±2.1	100.0±0.0	72.9±4.2 ***
	100.0±0.0	100.0±0.0	100.0±0.0	97.9±2.1	100.0±0.0	72.9±5.5 ***
Hatching rate	0.0±0.0	0.0±0.0	0.0±0.0	0.0±0.0	0.0±0.0	0.0±0.0
	0.0±0.0	16.7±2.1 ***	18.8±9.5 ***	0.0±0.0	0.0±0.0 *	2.1±2.1
	95.8±4.2	100.0±0.0 *	100.0±0.0	97.9±2.1	20.8±12.7 ***	14.6±5.5 ***
Malformation rate	0.0±0.0	0.0±0.0	0.0±0.0	2.1±2.1	2.1±2.1	25.0±3.6 ***
	0.0±0.0	2.1±2.1	0.0±0.0	8.3±2.1 **	2.1±2.1	37.5±6.3 ***
	3.3±3.3	0.0±0.0 *	0.0±0.0	2.1±2.1	2.1±2.1	27.1±5.5 ***

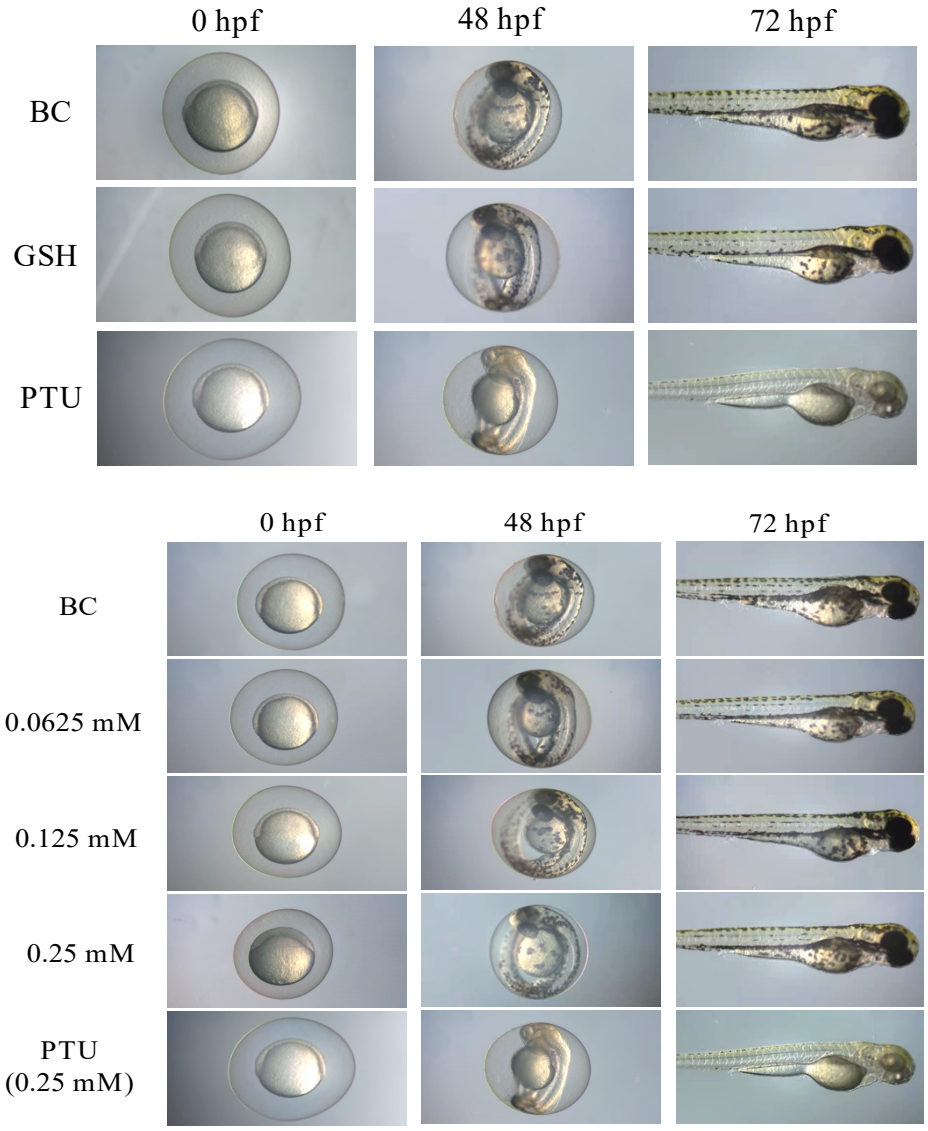

Fig. S2. Survival, hatching and malformation rate. (A) GSH solutions with different concentrations of survival, hatching and malformation rate. (B) PG solutions with different concentrations of survival, hatching and malformation rate.

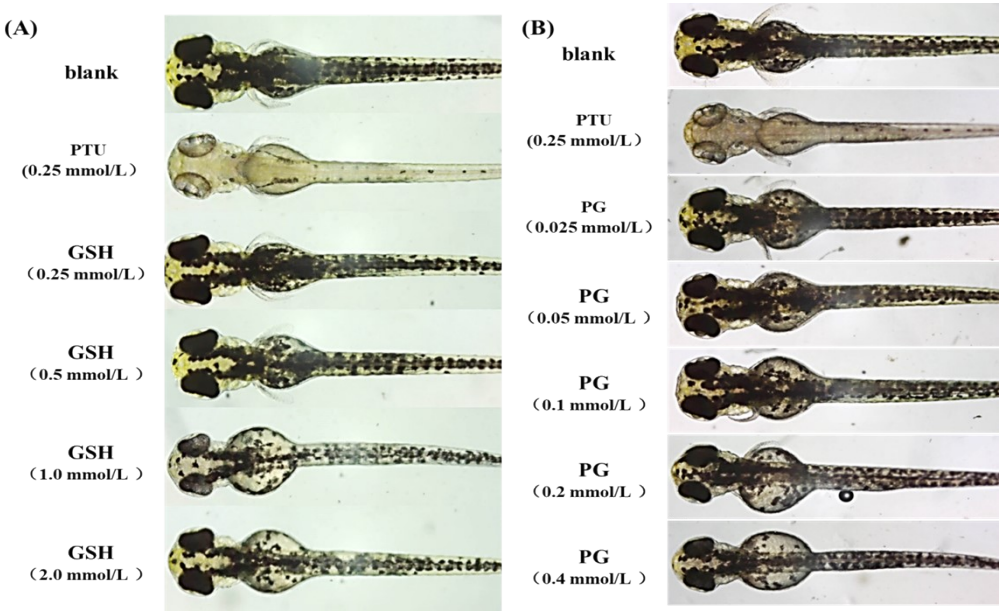

Fig. S3. Quantitative analysis of inhibition of melanin formation by GSH and PG in zebrafish. (A) GSH solutions with different concentrations were added into 8 hpf healthy embryos. (B) PG solutions with different concentrations were added into 8 hpf healthy embryos.

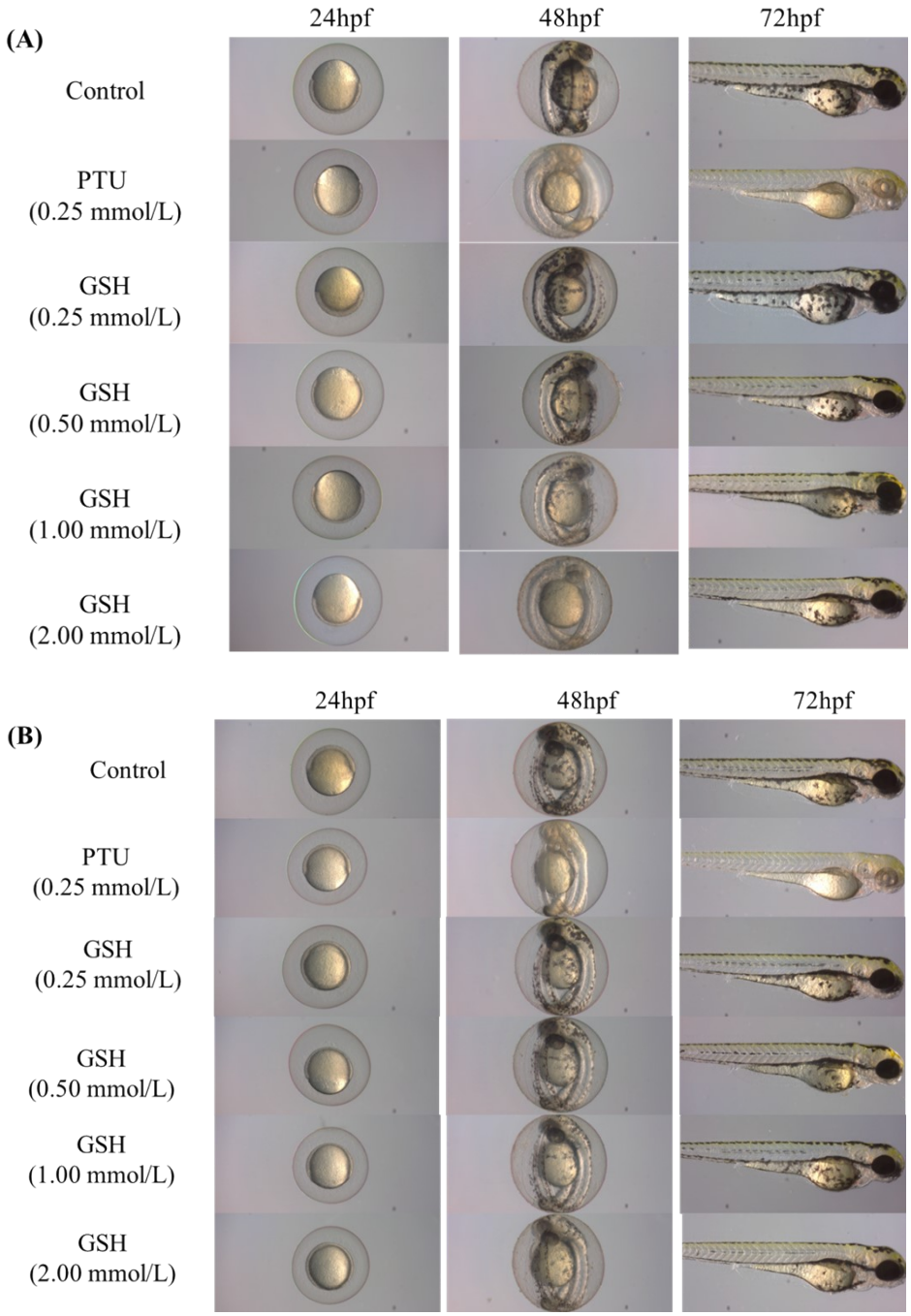
(A)
24hpf
48hpf
72hpf
Control
PTU
(0.25 mmol/L)
GSH
(0.25 mmol/L)
GSH
(0.50 mmol/L)
GSH
(1.00 mmol/L)
GSH
(2.00 mmol/L)
(B)
24hpf
48hpf
72hpf
Control
PTU
(0.25 mmol/L)
GSH
(0.25 mmol/L)
GSH
(0.50 mmol/L)
GSH
(1.00 mmol/L)
GSH
(2.00 mmol/L)

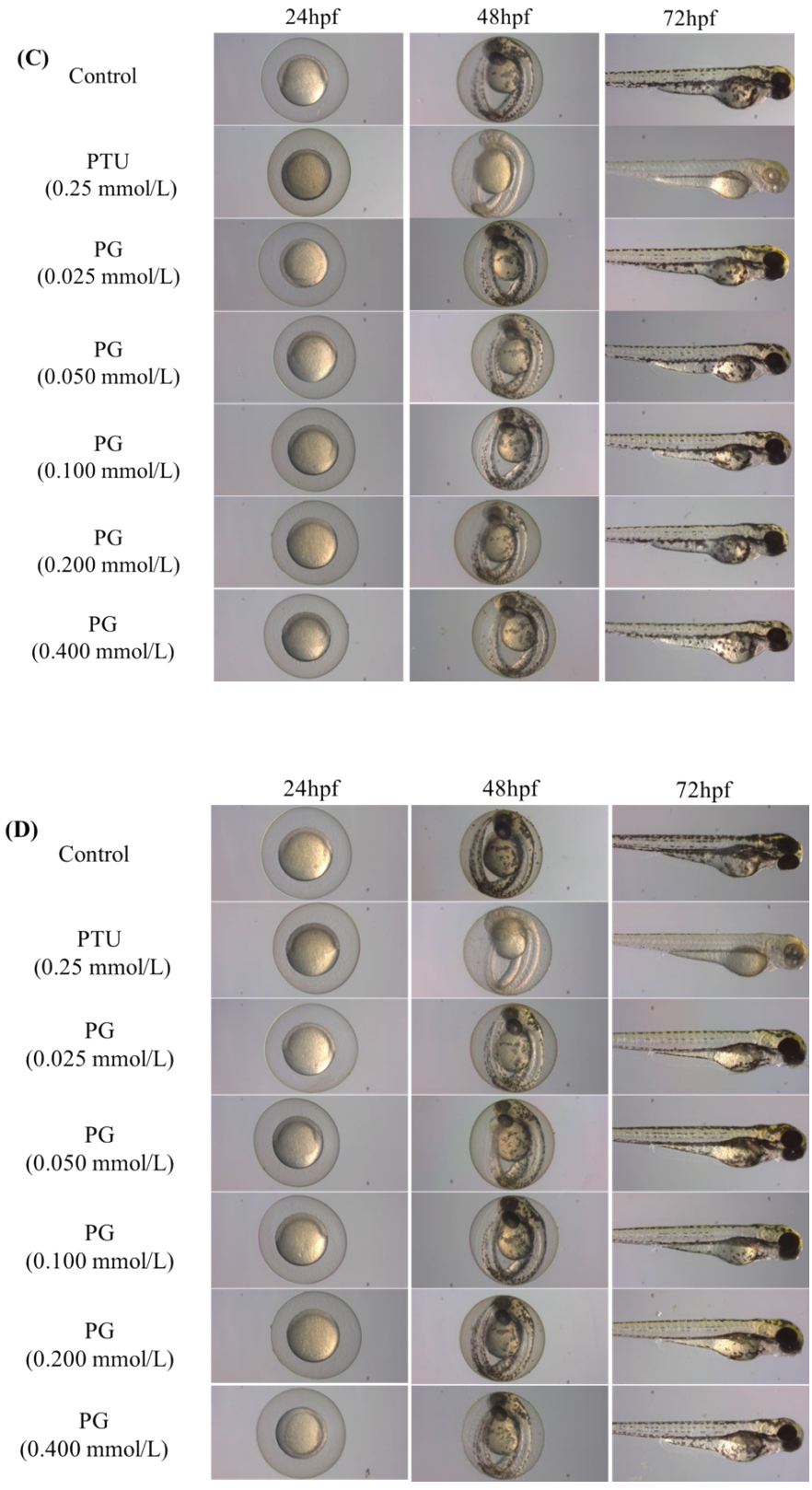

Fig. S4. Zebrafish melanin repair by itself at day-night. (A-B) GSH solutions with different concentrations were added in the light and dark. (C-D) PG solutions with different concentrations were added in the light and dark.

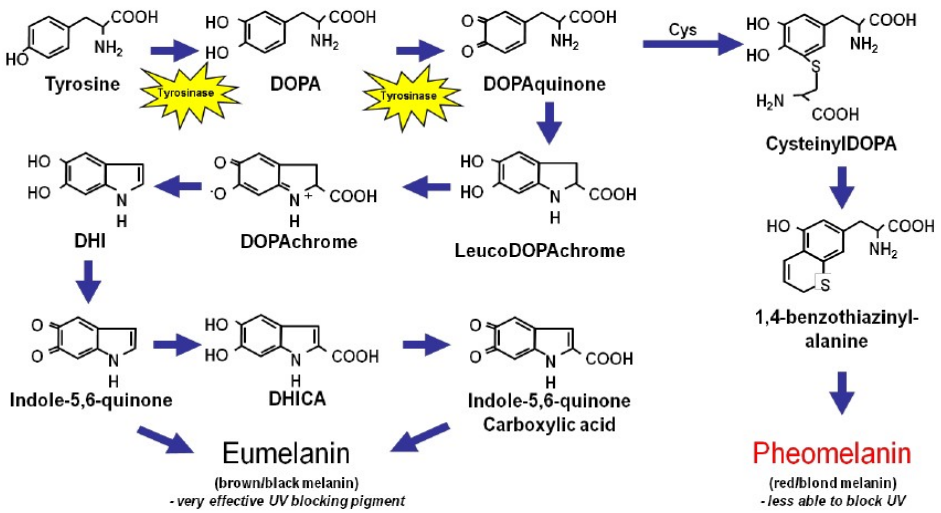

Fig.S5. Schematic representation of the melanogenesis pathway for eumelanin and Pheomelanin.

(Copy Right: John D'Orazio, Stuart Jarrett, Alexandra Amaro-Ortiz and Timothy Scott, *Int. J. Mol. Sci*. 2013, 14, 12222-12248)

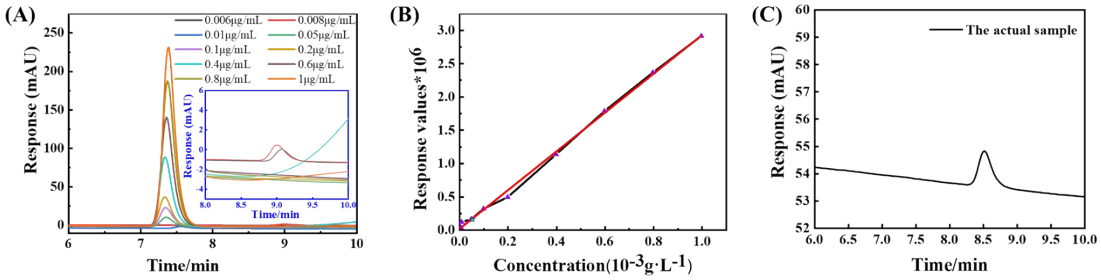

Fig. S6. HPLC of standard curve of L-DOPA. (A) L-DOPA standard curve. (B) L-DOPA linear fitting curve. (C) The actual sample was detected by HPLC.

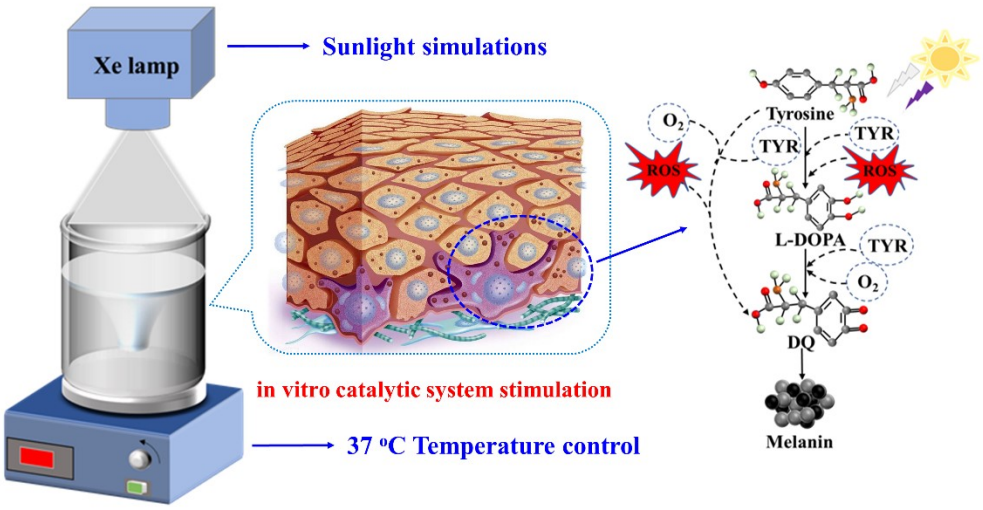

Figure S7 In vitro simulation of melanin production

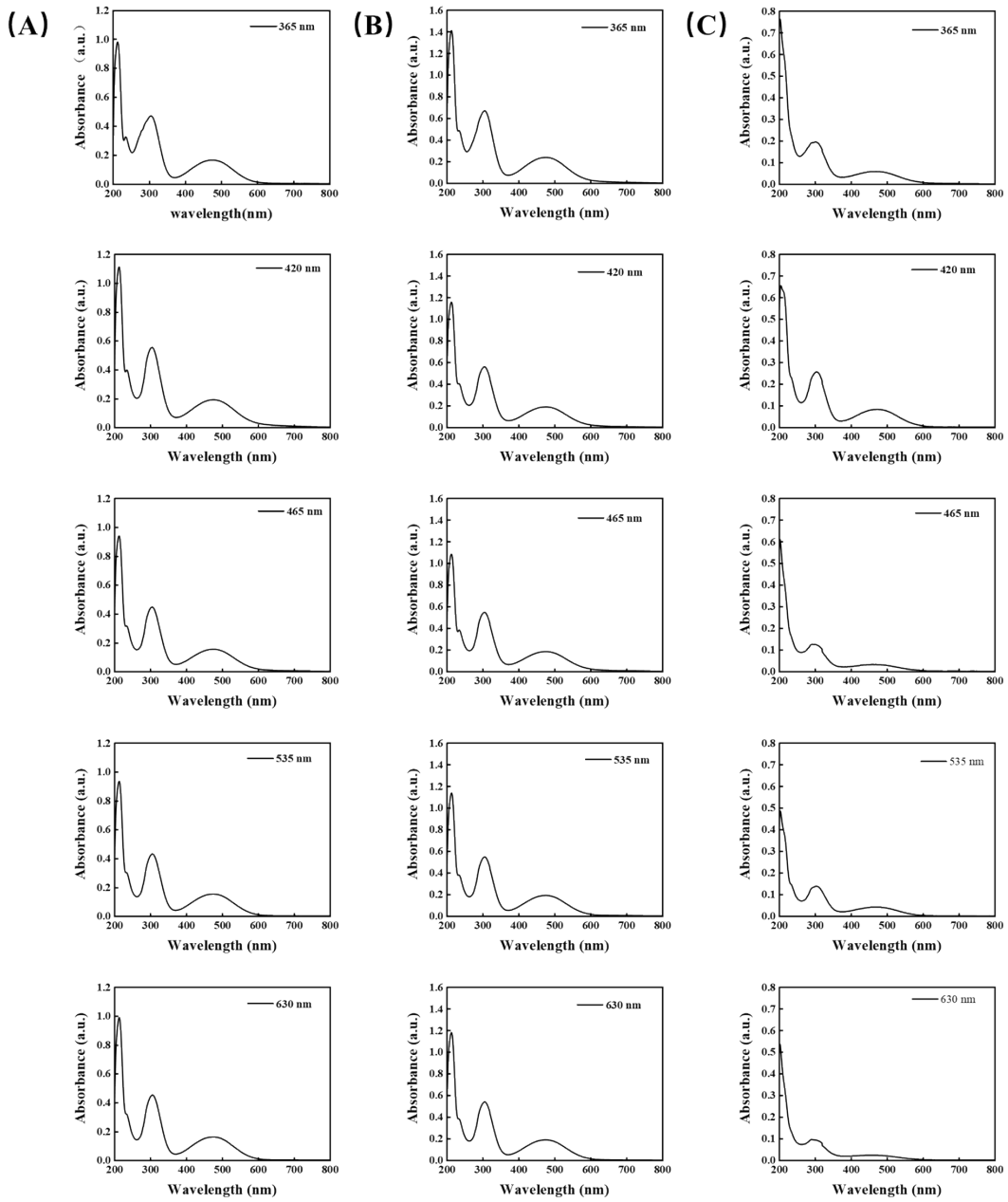

Figure S8 Effects of different wavelength light sources on melanin formation rate under air saturation, oxygen saturation and nitrogen saturation conditions. (A) Air saturation. (B) O_2 saturation. (C) N_2 saturation

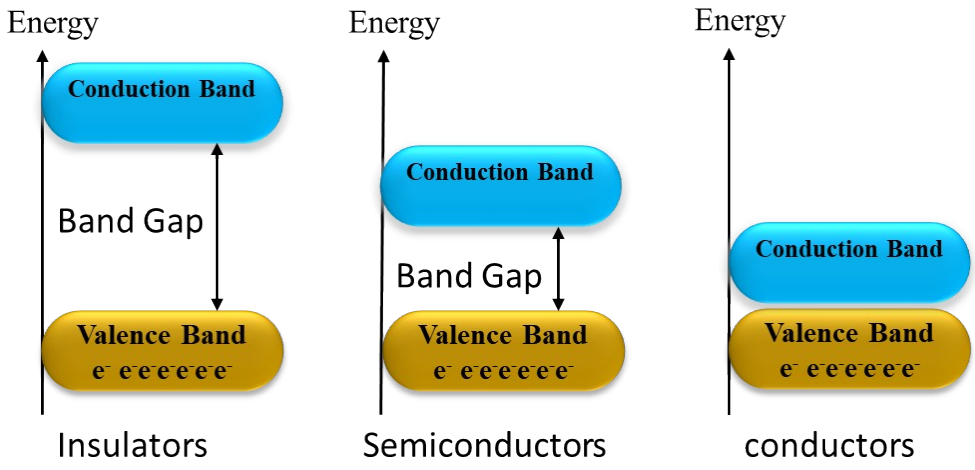

Fig.S9. Schematic diagram showing different valence and conduction band for Metal, Semiconductor, and insulating materials.

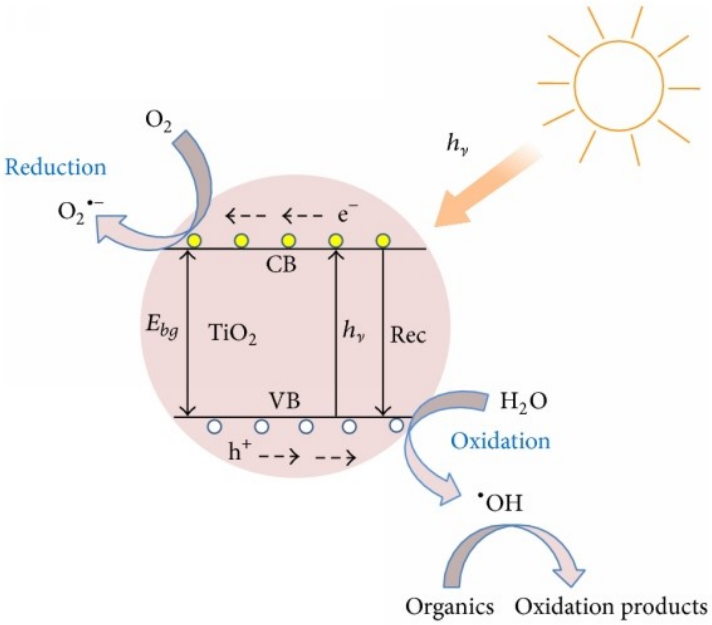

Fig.S10. General mechanism of TiO_2 in solar photocatalysis process. (h^+ = holes, e^- = electrons, $O_2^{\bullet-}$ = superoxide anion radical, O_2 = oxygen, • OH= hydroxide radical, OH^- = hydroxide).

(Copy Right: Tong Zhang et al, *International Journal of Photoenergy*, 12, (2014) 607954)